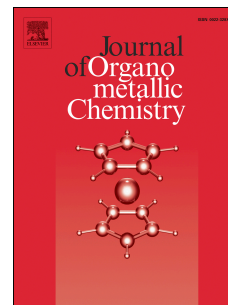# Accepted Manuscript

Synthesis and catalytic activity of nickel(II) complexes containing NCN pincer ligands

Ashwin G. Nair, Roy T. McBurney, Mark R.D. Gatus, D.Barney Walker, Mohan Bhadbhade, Barbara A. Messerle

Please cite this article as: A.G. Nair, R.T. McBurney, M.R.D. Gatus, D.B. Walker, M. Bhadbhade, B.A. Messerle, Synthesis and catalytic activity of nickel(II) complexes containing NCN pincer ligands, *Journal of Organometallic Chemistry* (2017), doi: 10.1016/j.jorganchem.2017.02.025.

X = Cl or Br

Ni(II) Pincer catalyst
2 mol%

THF, 4 h, 25 °C

Ni(II) Pincer Catalyst

**10 examples
up to >99% conversion**

Synthesis and Catalytic Activity of Nickel(II) Complexes Containing NCN Pincer Ligands

Ashwin G. Nair,[a] Roy T. McBurney,[a] Mark R. D. Gatus,[a] D. Barney Walker,[a] Mohan Bhadbhade[b] and Barbara A. Messerle[a, *]

[a] Department of Chemistry and Biomolecular Sciences, Macquarie University, Sydney 2109, Australia

[b] Mark Wainwright Analytical Centre, University of New South Wales, Sydney 2052, Australia

[*] Corresponding author

E-mail address: barbara.messerle@mq.edu.au (B. Messerle)

Abstract

In this study, nickel(II) complexes $[\mathbf{L^{me}Ni(II)Cl}]^+(BPh_4)^-$, $[\mathbf{L^{me}Ni(II)Cl}]^+(PF_6)^-$ and $[\mathbf{L^{et}_2Ni(II)}]^+(BPh_4)^-_2$ were synthesised and characterised in the solution and solid states. Ligands $\mathbf{L^{me}}$ ($C_{11}H_{12}N_6$) and $\mathbf{L^{et}}$ ($C_{13}H_{17}N_6$) featured a central carbene donor linked to pendant pyrazoles *via* either methylene or ethylene linkers. The catalytic activity of all three complexes was tested in the Kumada cross coupling reaction between phenylmagnesium bromide and aromatic halogen substituted substrates. $[\mathbf{L^{me}Ni(II)Cl}]^+(BPh_4)^-$ was found to be the most active catalyst.

Keywords

Nickel(II) pincer complexes

Organometallic catalysis

Kumada cross coupling

Graphical Abstract Synopsis

A square-planar Ni(II) pincer complex based on a carbene-bis-pyrazole ligand was found to be an effective catalyst for the Kumada cross coupling of phenylmagnsesium bromide with aryl halides at room temperature. Synthesis, structural characterization and catalysis behavior of this Ni(II) complex and related complexes was studied.

1. Introduction

Among the first reported catalytic C-C bond formation reactions was the Kumada cross coupling reaction.[1-3] The reaction involves the catalysed cross coupling between a Grignard reagent and an organic halide, which results in the formation of a new C-C bond. Despite the advent of alternative reactions, such as Suzuki,[4] Negishi,[5, 6] Stille[7-9] or Sonogashira[10] coupling reactions, Kumada cross coupling reactions continue to be used in industry due to the ability of the reaction to directly couple Grignard reagents to a wide variety of halide containing compounds.[11-13] The Kumada cross coupling is not limited to sp^2-hybridised carbons and hence has a greater versatility compared to other C-C coupling reactions.[14] Also, this reaction has a other advantages that make it an attractive tool for synthesis: it avoids the use of toxic organotin compounds utilised in Stille couplings; nickel(II) complexes are typically utilised as catalysts providing a reduced cost alternative for the same organic transformation compared to palladium; the thermal stability of Grignard reagents allows a greater range of reaction temperatures to be used for the successful coupling of both activated and deactivated substrates.[15, 16]

Significant attention has focused on transition metal complexes containing pincer ligands[17] as catalysts for C-C cross coupling reactions as these complexes can exhibit higher reactivity and increased stability over complexes containing bidentate or monodentate ligands.[18-20] Ni(II) complexes containing pincer ligands are widely used in C-C cross coupling reactions, particularly the coupling of aryl Grignards with aryl or alkyl halides.[21] The ability of the complexes bearing pincer ligands to efficiently catalyse Kumada cross coupling reactions depends on factors such as the degree of electron donation to the metal centre, and the lability of the coordinating groups to the

metal centre.[11] Only a few complexes containing a central *N*-heterocyclic carbene (NHC) donor and labile donor arms have been reported in the literature, see Fig. 1.[22-25]
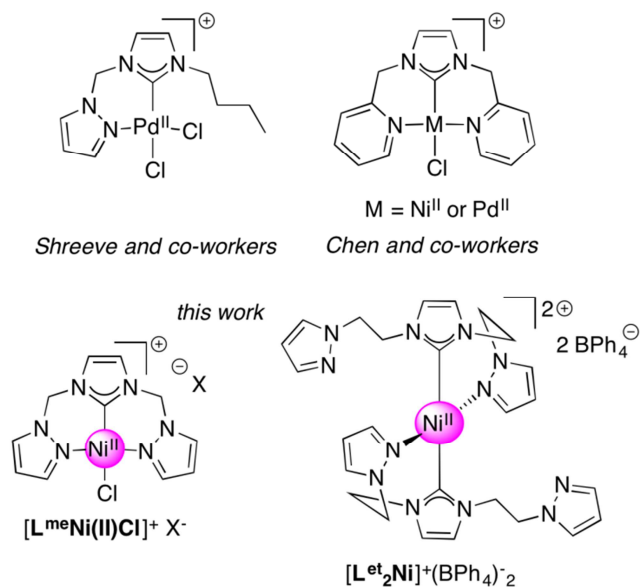
Fig. 1 Catalysts featuring ligands containing a central carbene donor and hemilabile pendant donors and the Ni(II) catalysts presented in this work.

In this work, two pro-ligands bearing a central carbene unit flanked by pyrazole pendant donor arms were coordinated to nickel(II), generating three novel Ni(II) complexes and their coordination chemistry was explored in the solution and solid states, see Fig. 1. The ligands differed in only the length of their linker between imidazole arm and pyrazole arms, pro-ligand $\mathbf{L^{me}H}$ possessed a methylene bridge, whereas $\mathbf{L^{et}H}$ possessed an ethylene bridge. We have successfully used Rh(I), Ir(I) and Ru(II) complexes containing these ligands for catalysis.[24, 25] The catalytic activity of all three Ni(II) complexes was investigated in the Kumada cross coupling of phenyl magnesium bromide with aryl halogens.

2. Experimental

2.1 Materials

All manipulations were carried out under a nitrogen atmosphere using standard Schlenk techniques or in a nitrogen or argon filled glovebox unless otherwise stated. Imidazolium pro-ligands $\mathbf{L^{me}H}$ and

L^{et}H,[24] [**L^{me}₂Ag(I)**]⁺(BPh₄)⁻ [25] were prepared according to the literature methods. Commercially available reagents were purchased from Sigma-Aldrich or Alfa Aesar Inc. and used as received. Dichloromethane and acetonitrile were dried using a solvent purification system. Tetrahydrofuran used for catalysis reactions was distilled and dried using a sodium mirror and stored under an inert atmosphere. All catalysis substrates were purified by distillation and glassware was oven-dried (120-150 °C) prior to use.

2.2 Equipment

NMR spectra were recorded on a Bruker Avance III 500 MHz and 600 MHz spectrometers. Chemical shifts (δ) are quoted in ppm and referenced to residual solvent resonances. Mass spectra were acquired using a Thermo Scientific LCQ Fleet (ESI-MS) mass spectrometer, or using a Thermo Scientific LTQ Orbitrap XL instrument at the Bioanalytical Mass Spectrometry Facility at University of New South Wales. 'M' is defined as the molecular weight of the compound or cationic fragment of interest. IR spectra were recorded as KBr discs using an Avatar 370 FTIR spectrometer at the University of New South Wales. Elemental analyses were carried out at the Campbell Microanalytical Labaoratory, University of Otago, New Zealand, Elemental Analysis Unit, The Research School of Chemistry, Australian National University and the Elemental Microanalysis Service at the Department of Chemistry and Biomolecular Sciences, Macquarie University. Single crystal X-ray analyses were carried out at the Mark Wainwright Analytical Centre, University of New South Wales, Sydney. X-ray diffraction measurements were carried out on a Bruker Kappa APEXII CCD diffractometer using graphite-monochromated Mo-Kα radiation (λ = 0.710723 Å). All structures were solved by direct methods and the full-matrix least-square refinements were carried out using SHELXL. Absorption correction was performed using Multi-scan SADABS and H-atom parameters were treated as constrained. CCDC 1513714-1513716 contains supplementary X-ray crystallographic data for complexes [**L^{me}Ni(II)Cl**]⁺(BPh₄)⁻, [**L^{me}Ni(II)Cl**]⁺(PF₆)⁻ and [**L^{et}₂Ni(II)**]⁺(BPh₄)⁻₂.

2.3   General Procedure for Kumada Cross Couplings

Nickel(II) complexes were pre-dried under vacuum prior to catalysis reactions. The Kumada cross coupling experiments were carried out under standard Schlenk conditions and performed in duplicate with the results averaged. GC-MS analyses were performed on a Shimadzu QP2010 Plus gas chromatograph-mass spectrometer. A BP20 column was used, and the oven temperature was ramped from 50 to 220 °C at a rate of 10 °C min^{-1}. UHP grade helium was used as the carrier gas. The screw-cap autosampler vials used were obtained from Agilent Technologies and were fitted with PTFE/silicone septa and 0.2 mL micro inserts. The identification of products was confirmed using GC-MS spectroscopy and ^{1}H NMR spectroscopy and the conversion of substrate to product(s) was monitored by GC-MS by comparing the peak areas of the product(s) to starting materials. A typical catalysed Kumada coupling experiment was performed as follows: a Schlenk flask was charged with the catalyst (2 mol%) to which 10 mL of THF was cannulated in an inert atmosphere. The organohalide substrate (0.5 mmol) and phenylmagnesium bromide (1.5 mmol) were added subsequently using an air tight syringe. The mixture was stirred at 25 °C for 4 hours. Aliquots were taken at regular intervals, which were quenched with cold deionised H_2O (1 mL) followed by the addition of Et_2O (1 mL). The organic phase was extracted, dried using anhydrous $MgSO_4$ and filtered using a plug of silica. The crude products (2-3 drops of the Et_2O phase) were diluted in 1 mL of dichloromethane and collected for GC-MS analysis. The organic layers of selected reactions were also reduced to dryness under vacuum, dissolved in $CDCl_3$ and analysed using ^{1}H NMR spectra.

2.4   Synthesis

2.4.1   Synthesis of [L^{me}Ni(II)Cl]$^+$(BPh$_4$)$^-$

[L^{me}$_2$Ag(I)]$^+$(BPh$_4$)$^-$ (0.050 g, 0.056 mmol) and Ni(PPh$_3$)$_2$Cl$_2$ (0.077 g, 0.118 mmol) were dissolved in 20 mL of dry THF. The mixture was left stirring overnight at room temperature under an N$_2$ atmosphere. The resulting yellow mixture was filtered using glass fibre (GF/C) filter paper and the

filtrate reduced to 10 mL. 40 mL of diethyl ether was slowly added to the solution to precipitate [L^{me}Ni(II)Cl]$^+$(BPh$_4$)$^-$ as a yellow powder. Crystals suitable for X-ray crystallography were grown by vapour diffusion of diethyl ether into a saturated acetone (2 mL) solution of [L^{me}Ni(II)Cl]$^+$(BPh$_4$)$^-$. Yield: 40%. ^{1}H NMR (600 MHz, (CD$_3$)$_2$CO): δ 8.29 (br d, 2H, H^3), 8.18 (br d, 2H, H^5), 7.70 (br s, 2H, H^1), 7.37-7.30 (m, 8H, *o*-BPh$_4$), 6.92 (t, ^3J= 7.3 Hz, 8H, *m*-BPh$_4$), 6.95 (t, ^3J= 7.3 Hz, 4H, *p*-BPh$_4$) 6.81 (br d, 4H, H^2), 6.58 (m, 2H, H^4). ^{13}C{^{1}H} NMR (150 MHz, (CD$_3$)$_2$CO): δ 164.3-163.3 (C ipso of BPh$_4$), 147.6 (C3), 143.9 (C6), 136.9 (C1), 136.0 (*o*-C of BPh$_4$), 125.6 (*m*-C of BPh$_4$), 121.8 (*p*-C of BPh$_4$), 122.0 (C5), 107.6 (C2), 61.9 (C4) ppm. Elemental analysis found: C, 65.54; H, 5.07; N, 13.04. Calc. for NiC$_{35}$H$_{32}$B N$_6$Cl: C, 65.52; H, 5.03; N, 13.10. ESI-MS (*m/z* = 303.05) [M-Cl+OH]$^+$.

2.4.2 Synthesis of [L^{me}Ni(II)Cl]$^+$(PF$_6$)$^-$

[L^{me}H.]$^+$(PF$_6$)$^-$ (0.090 g, 0.242 mmol) and Ag$_2$O (0.150 g, 0.640 mmol) were mixed in 30 mL of dry CH$_2$Cl$_2$ and the mixture was left stirring overnight at room temperature under an N$_2$ atmosphere. Filtration of the dark mixture using glass fibre (GF/C) filter paper gave a colourless filtrate which was reduced to dryness. The resulting white powder was redissolved in 30 mL of dry THF to which Ni(PPh$_3$)$_2$Cl$_2$ (0.158 g, 0.242 mmol) was added. The orange suspension was left stirring overnight at room temperature under an N$_2$ atmosphere. The resulting yellow solution was filtered using glass fibre (GF/C) filter paper and the filtrate reduced to 10 mL. 40 mL of diethyl ether was slowly added to the solution to precipitate [L^{me}Ni(II)Cl]$^+$(PF$_6$)$^-$ as a yellow powder. Crystals suitable for X-ray crystallography were grown by vapour diffusion of diethyl ether into a saturated acetone (2 mL) solution of [L^{me}Ni(II)Cl]$^+$(PF$_6$)$^-$. Yield: 62%. ^{1}H NMR (600 MHz, (CD$_3$)$_2$CO): δ 8.36 (br d, 2H, H^3), 8.16 (br d, 2H, H^5), 7.79 (br s, 2H, H^1), 6.92 (br d, 4H, H^2), 6.60 (m, 2H, H^4). ^{13}C{^{1}H} NMR (150 MHz, (CD$_3$)$_2$CO): δ 147.6 (C3), 143.9 (C6), 136.9 (C1), 122.0 (C5), 107.6 (C2), 61.9 (C4) ppm. Elemental analysis found: C, 28.24; H, 2.52; N, 17.90. Calc. for Ni1C$_{11}$H$_{12}$PN$_6$F$_6$Cl: C, 28.27; H, 2.59; N, 17.98. ESI-MS (*m/z* = 303.05) [M-Cl+OH]$^+$.

2.4.3 Synthesis of $[\mathbf{L^{et}_2Ni(II)}]^+(BPh_4)^-_2$

$[\mathbf{L^{et}H}]^+(BPh_4)^-$ (0.100 g, 0.242 mmol) and potassium bis(trimethylsilyl)amide (0.150 g, 0.640 mmol) and $Ni(PPh_3)_2Cl_2$ (0.158 g, 0.242 mmol) were mixed in 30 mL of dry THF and the resulting yellow mixture was left stirring overnight at room temperature under an N_2 atmosphere. The resulting yellow solution was filtered using glass fibre (GF/C) filter paper and the filtrate reduced to 10 mL. 40 mL of diethyl ether was slowly added to the solution to precipitate $[\mathbf{L^{et}_2Ni(II)}]^+(BPh_4)^-_2$ as a yellow powder. Crystals suitable for X-ray crystallography were grown by vapour diffusion of diethyl ether into a saturated acetone (2 mL) solution of $[\mathbf{L^{et}_2Ni(II)}]^+(BPh_4)^-_2$. Yield: 18%. ^{1}H NMR (600 MHz, $(CD_3)_2CO$): δ 8.11 (d, ^2J = 2.3 Hz, 2H, H^{13}), 7.98 (br t, 2H, H^{9a}), 7.84 (br d, 2H, H^1), 7.60 (d, ^2J = 2.3 Hz, 2H, H^{11}), 7.53(d, ^2J = 2.2 Hz, 2H, H^8), 7.49 (br d, 2H, H^6), 7.47 (d, ^2J = 2.2 Hz, 2H, H^3), 7.35-7.29 (m, 8H, *o*-BPh$_4$), 6.94 (t, ^3J= 7.3 Hz, 8H, *m*-BPh$_4$), 6.80 (t, ^3J= 7.3 Hz, 4H, *p*-BPh$_4$), 6.42 (dd, ^3J = 2.2 Hz 4H, H^{12}), 6.16 (br m, 2H, H^2), 5.61(br d, 2H, H^{10a}), 5.58 (br d, 2H, H^{10b}), 5.04 (br m, 2H, H^{4a}), 4.88 (br m, 2H, H^{9b}), 4.63 (br m, 2H, H^{4b}), 4.37 (br m, 2H, H^{5a}), 4.29 (br m, 2H, H^{5b}). ^{13}C{^{1}H} NMR (150 MHz, $(CD_3)_2CO$): δ 151.7 (C7), 147.6 (C3), δ142.5 (C11), 141.9 (C1), 140.8 (C10), 136.0 (*o*-C of BPh$_4$), 135.0 (C13), 131.1 (C3), 127(C8), 125.6 (*m*-C of BPh$_4$), 123.5 (C6), 121.8 (*p*-C of BPh$_4$), 108.9 (C12), 105.5 (C2), 50.6 (C5), 50.0 (C4), 49.4 (C9), 48.7 (C10) ppm. Elemental analysis found: C, 72.07; H, 5.97; N, 13.04. Calc. for $Ni_1C_{74}H_{72}B_2N_{12}$: C, 73.47; H, 6.00; N, 13.89. ESI-MS: (*m/z* = 889.4) [M+BPh$_4$]$^+$.

3. Results and Discussion

3.1 Synthesis and characterisation of $[\mathbf{L^{me}Ni(II)Cl}]^+(BPh_4)^-$

Pro-ligands $\mathbf{L^{me}H}$ and $\mathbf{L^{et}H}$ were previously synthesised in our group.[24] The Ni(II) complex of the $\mathbf{L^{me}}$ pincer ligand was synthesised by *in situ* silver complexation followed by transmetallation with nickel(II).[25] Pro-ligand $[\mathbf{L^{me}H}]^+(BPh_4)^-$ was first treated with an excess of silver(I) oxide in dichloromethane to generate $[\mathbf{L^{me}_2Ag(I)}]^+(BPh_4)^-$ *in situ* prior to treatment with two

molar equivalents of $Ni(PPh_3)_2Cl_2$ to yield complex $[\textbf{L}^{\textbf{me}}\textbf{Ni(II)Cl}]^+(BPh_4)^-$ as a yellow micro-crystalline solid in 40% yield (Scheme 1a). Column chromatography only yielded one fraction that was clearly identifiable as the Ni(II) complex, the rest proved to be an intractable mixture. Multiple attempts were made to increase the yield of complex $[\textbf{L}^{\textbf{me}}\textbf{Ni(II)Cl}]^+(BPh_4)^-$, such as using other Ni(II) salts or an external base (Et$_3$N). Whilst complex $[\textbf{L}^{\textbf{me}}\textbf{Ni(II)Cl}]^+(BPh_4)^-$ could be synthesised using a base, the yield did not improve.
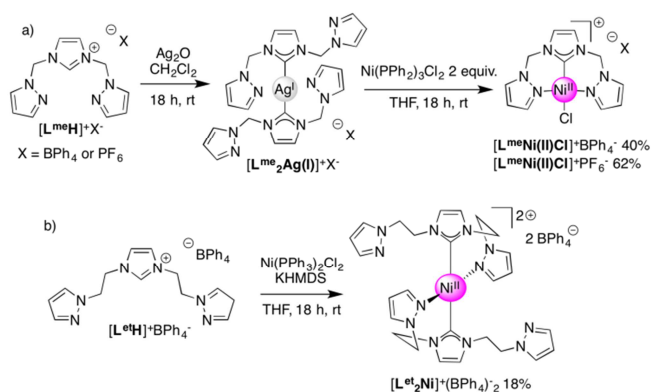
**Scheme 1** Synthesis of complexes (a) $[\textbf{L}^{\textbf{me}}\textbf{Ni(II)Cl}]^+X^-$ (where X = BPh$_4$ or PF$_6$) and (b) $[\textbf{L}^{\textbf{et}}_2\textbf{Ni(II)Cl}]^+(BPh_4)^-_2$.

The ^{1}H NMR spectrum of complex $[\textbf{L}^{\textbf{me}}\textbf{Ni(II)Cl}]^+(BPh_4)^-$ exhibited broad resonances for all hydrogens attributed to the pincer ligand at room temperature. A single set of aromatic resonances between 7.5 and 8.4 ppm were attributed to the pyrazolyl and carbene donors. The low number of resonances indicated that the complex had a plane of symmetry through the carbene-Ni-Cl axis, with the ligand likely coordinated in a tridentate fashion to Ni(II) through all three donors (κ_3-*NCN*). There were significant differences between the chemical shifts of the resonances due to pyrazolyl hydrogens of the Ni(II) complex in comparison to those observed for the analogous silver(I) intermediate. The pyrazolyl resonances of intermediate $[\textbf{L}^{\textbf{me}}_2\textbf{Ag(I)}]^+(BPh_4)^-$ occurred at 7.60 ppm and 8.13 ppm, whereas the pyrazole resonances of the $[\textbf{L}^{\textbf{me}}\textbf{Ni(II)Cl}]^+(BPh_4)^-$ occurred at 8.26 ppm and 8.29 ppm respectively. The downfield shift of the pyrazolyl resonances of $[\textbf{L}^{\textbf{me}}\textbf{Ni(II)Cl}]^+(BPh_4)^-$ indicated that the transmetallation reaction resulted in coordination of the two pyrazolyl ligand arms

to the Ni(II) centre, unlike in [**L^{me}$_2$Ag(I)**]$^+$(BPh$_4$)$^-$ where the *N*-donors remain unbound. The integration ratios of ligand proton resonances to those of the BPh$_4$ counterion demonstrated that the ratio of ligand to counterion was 1:1. As the ^{1}H NMR spectrum indicates that all ligand donors are bound to the metal centre, it is highly likely that a Cl co-ligand is also bound to the Ni(II) centre. ^{13}C{^{1}H} NMR and 2D NMR spectroscopy did not reveal any valuable information that explained the broad signals in the ^{1}H NMR spectrum. There are different possibilities for the broad signals in the NMR spectrum including purity, paramagnetism and conformational flexibility of the complex [**L^{me}Ni(II)Cl**]$^+$(BPh$_4$)$^-$ in solution state. Further characterisation was therefore carried out to identify the cause of the broad signals in the NMR spectrum.

Crystals suitable for X-ray analysis were grown by vapour diffusion of diethyl ether into a saturated solution of [**L^{me}Ni(II)Cl**]$^+$(BPh$_4$)$^-$ in acetone. X-ray crystal structure analysis of [**L^{me}Ni(II)Cl**]$^+$(BPh$_4$)$^-$ showed that Ni(II) had a square-planar geometry, with the ligand **L^{me}** coordinated in a tridentate fashion *via* its NCN donors as expected (Fig. 2). The central NHC is twisted out of the square plane, such that the two methylene linkers are positioned on opposite faces of the plane at a torsion angle of 30.1^o. Mass spectrometry and elemental analysis of crystals of [**L^{me}Ni(II)Cl**]$^+$(BPh$_4$)$^-$ showed it to be pure. However, ^{1}H NMR analysis of the isolated crystals used for solid state structure determination of [**L^{me}Ni(II)Cl**]$^+$(BPh$_4$)$^-$ and elemental analysis produced a spectrum identical to that obtained for the previously synthesised yellow powder with broad signals. This evidence indicated that the broad resonances in the NMR spectrum of [**L^{me}Ni(II)Cl**]$^+$(BPh$_4$)$^-$ was not due to the presence of impurities.
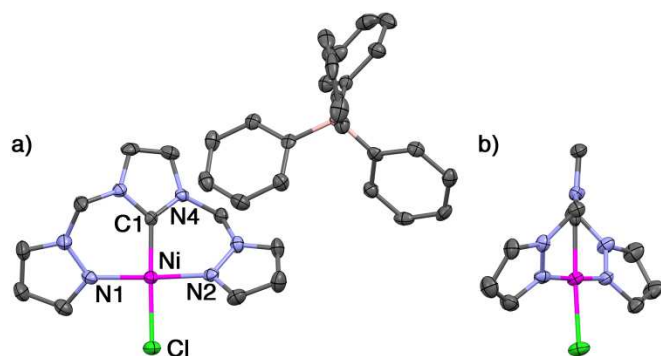
Fig. 2. X-ray crystal structure of (**L^me^Ni(II)Cl**]^+^(BPh₄)^-^ as viewed (a) front on and (b) side on. Ellipsoids are shown at 50% probability level, hydrogens are omitted for clarity, BPh₄ anion is omitted in (b).

As we observed in previous work, facial coordination of ligand **L^me^** to Ru(II) is possible.[25] Complex [**L^me^Ni(II)Cl**]^+^(BPh₄)^-^ could therefore exist in an equilibrium between square planar and tetrahedral conformations (Fig. 3) which could lead to broadened signals in the ^{1}H NMR spectrum due to the contribution of a tetrahedral paramagnetic nickel(II) species. The Ni(PPh₃)₂Cl₂ precursor used for the synthesis of [**L^me^Ni(II)Cl**]^+^(BPh₄)^-^ itself exists in such an equilibrium.[26, 27] Analysis of complex [**L^me^Ni(II)Cl**]^+^(BPh₄)^-^ in acetone solution using UV/Vis spectroscopy revealed the presence of only one strong signal at 460 nm which is characteristic of a square planar Ni(II) compound.[28] Evan's method using ^{1}H NMR at 25 °C demonstrated that there were no paramagnetic nickel(II) species present.[29, 30] These results confirmed that the broadness observed in the 1H NMR spectrum was not due to paramagnetism.
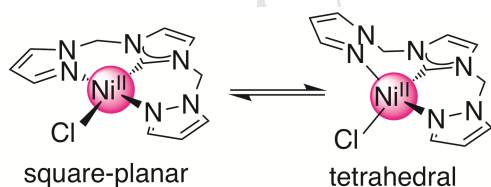
**Fig. 3.** Proposed equilibrium reaction between the square planar and tetrahedral conformations of complex [**L^me^Ni(II)Cl**]^+^(BPh₄)^-^.

To test our last remaining hypothesis that broadness of the ^{1}H NMR spectrum is due to the flexible ligand, $[\mathbf{L^{me}Ni(II)Cl}]^{+}(BPh_4)^{-}$ was analysed using variable temperature ^{1}H NMR spectroscopy (Fig. 4). Despite the resonances not completely sharpening up at the lower temperature they did shift position; the ^{1}H NMR spectrum of complex $[\mathbf{L^{me}Ni(II)Cl}]^{+}(BPh_4)^{-}$ still showed the same number of resonances as observed at room temperature. It seems likely that the tridentate coordination of the ligand is preserved at the lower temperatures and that the broadness in the ^{1}H NMR spectrum of complex $[\mathbf{L^{me}Ni(II)Cl}]^{+}(BPh_4)^{-}$ is due to conformational flexibility of the complex arising from changes in the relative orientations of the pendant pyrazole arms of the ligand, see Fig. 5.
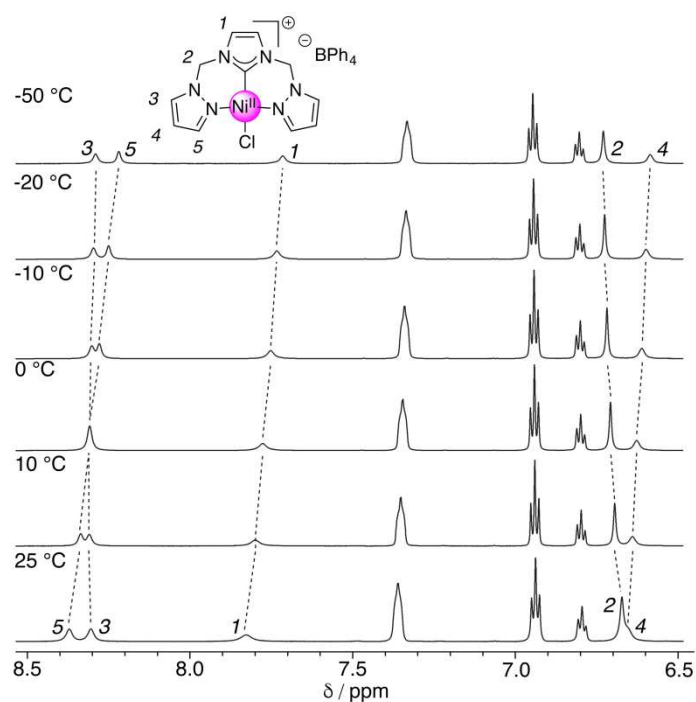
Fig. 4 Variable temperature NMR (600 MHz, $(CD_3)_2CO$) of complex $[\mathbf{L^{me}Ni(II)Cl}]^{+}(BPh_4)^{-}$. Assignments correspond to the labelling shown in the figure.
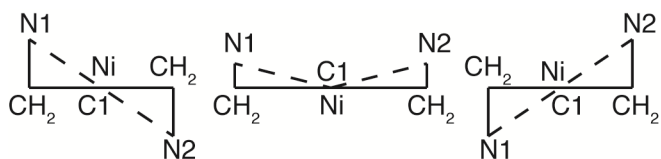
Fig. 5 Conformational flexibility arising from changes in the relative orientations of the pyrazole arms of complex [**L^{me}Ni(II)Cl**]⁺(BPh₄)⁻.

3.2   Synthesis and characterisation of [**L^{me}Ni(II)Cl**]⁺(PF₆)⁻

Complex [**L^{me}Ni(II)Cl**]⁺(BPh₄)⁻ proved to be difficult to synthesise in a reasonable yield, requiring a number of purification steps, and NMR characterisation of the product proved difficult. As the choice of counter ion used in a metal complex can often affect ease of synthesis and purification, and modify catalytic activity,[31] the analogous PF_6^- derivative of complex [**L^{me}Ni(II)Cl**]⁺(BPh₄)⁻ was synthesised. Pro-ligand [**L^{me}H**]⁺(PF₆)⁻ was synthesised following a similar method reported previously.[24] However, the counterion exchange reaction of the [**L^{me}H**]⁺Cl⁻ salt was performed with 1.2 equivalents of NH_4PF_6 instead of $NaBPh_4$. Pro-ligand [**L^{me}H**]⁺(PF₆)⁻ was isolated as a crystalline white solid in 56% yield. The ^1H NMR spectrum of [**L^{me}H**]⁺(PF₆)⁻ was analogous to that of [**L^{me}H**]⁺(BPh₄)⁻, exhibiting six ^1H resonances with the characteristic imidazolium hydrogen signal appearing in the expected region at 9.56 ppm. [**L^{me}H**]⁺(PF₆)⁻ was reacted with excess Ag_2O to produce [**L^{me}₂Ag(I)**]⁺(PF₆)⁻ as a pale brown solid (Scheme 1a), to which $Ni(PPh_3)_2Cl_2$ was added *in situ* to afford [**L^{me}Ni(II)Cl**]⁺(PF₆)⁻ as an orange powder in 62% yield. The ^1H NMR spectrum of [**L^{me}Ni(II)Cl**]⁺(PF₆)⁻ was similar to the analogous BPh₄ complex; the ^1H NMR spectrum of the PF_6^- complex exhibited five broad ligand resonances. Unfortunately, just as [**L^{me}Ni(II)Cl**]⁺(BPh₄)⁻ could not be characterized using ^{13}C NMR or 2D NMR techniques at 25 °C, neither could [**L^{me}Ni(II)Cl**]⁺(PF₆)⁻ as the resonances were too broad. Analysis of [**L^{me}Ni(II)Cl**]⁺(PF₆)⁻ using UV/Vis spectroscopy produced a single peak at 460 nm, similar to the UV/Vis spectrum of [**L^{me}Ni(II)Cl**]⁺(BPh₄)⁻ which suggested that the broadness was not a result of any paramagnetic species. Low temperature NMR spectroscopy at -50 °C allowed characterisation of the complex to be achieved using ^{13}C NMR and 2D NMR techniques. The ^1H NMR spectrum of [**L^{me}Ni(II)Cl**]⁺(PF₆)⁻ at room temperature indicated a tridentate coordination mode to a square planar Ni(II) centre, similar to of [**L^{me}Ni(II)Cl**]⁺(BPh₄)⁻. The only major difference between their ^1H NMR spectra was that the

resonances due to H^2 and H^4 are well separated in [**L^{me}Ni(II)Cl**]$^+$(PF$_6$)$^-$ compared to those of [**L^{me}Ni(II)Cl**]$^+$(BPh$_4$)$^-$, suggesting the change in counterion altered the chemical environment experienced by the ligand.

Crystals of [**L^{me}Ni(II)Cl**]$^+$(PF$_6$)$^-$ suitable for X-ray analysis were grown by vapour diffusion of diethyl ether into a saturated solution of [**L^{me}Ni(II)Cl**]$^+$(PF$_6$)$^-$ in acetone. Analysis using X-ray crystallography confirmed the expected κ_3-*NCN* symmetric structure with the Cl co-ligand terminally bound to the Ni(II) metal centre, in a *trans* position relative to the carbene (Fig. 6). Mass spectrometry shows a dominant signal at 303.05 *m/z* which was attributed to the cationic fragment [L^{me}Ni(II)OH]$^+$. The structure with the exemption of the counter ion proved to be isostructural to [**L^{me}Ni(II)Cl**]$^+$(BPh$_4$)$^-$.
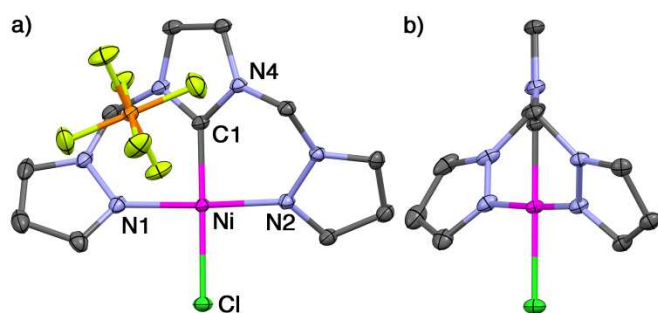
Fig. 6. X-ray crystal structure of complex [**L^{me}Ni(II)Cl**]$^+$(PF$_6$)$^-$ with ellipsoids at the 50% probability level, hydrogens have been omitted for clarity.

3.3   Synthesis and characterisation of [**L$^{et}_2$Ni(II)**]$^+$(BPh$_4$)$^-_2$

The use of a pincer ligand containing a longer alkyl linker between the central imidazolyl and pendant pyrazolyl moieties can affect the coordination of the ligand to a metal centre. Therefore, the pro-ligand [**L^{et}H**]$^+$(BPh$_4$)$^-$ with the ethylene linker between the carbene and pyrazole units was used.[24] As before, we opted for a silver transmetallation route to attempt to generate the final complex. Complex [**L$^{et}_2$Ag(I)**]$^+$(BPh$_4$)$^-$ was obtained as a white solid by reaction of ligand [**L^{et}H**]$^+$(BPh$_4$)$^-$ with excess Ag$_2$O. The ^{1}H NMR spectrum of the white solid contained nine proton resonances, six of which were attributed to the ligand protons and the remaining three resonances are

assigned to the BPh$_4$ protons. In a similar fashion to [**L$^{me}_2$Ag(I)**]$^+$(BPh$_4$)$^-$, the absence of the imidazolium proton resonance in the ^{1}H NMR spectrum of [**L$^{et}_2$Ag(I)**]$^+$(BPh$_4$)$^-$ indicated successful complexation of silver(I) to the ligand. The ratio of the integrals of the proton resonances indicate that the ligand to BPh$_4$ proton ratio is 2 : 1 which was indicative of a homoleptic structure for the silver complex [**L$^{me}_2$Ag(I)**]$^+$(BPh$_4$)$^-$. With the aim of synthesising a Ni(II) complex of ligand **L^{et}** two equivalents of Ni(PPh$_3$)$_2$Cl$_2$ were added to [**L$^{et}_2$Ag(I)**]$^+$(BPh$_4$)$^-$. However, the reaction of [**L$^{et}_2$Ag(I)**]$^+$(BPh$_4$)$^-$ and Ni(PPh$_3$)$_2$Cl$_2$ resulted in a mixture of unreacted starting material and insoluble silver salts. We attempted numerous repeats of this reaction, however all proved unsuccessful, hence this route was abandoned. An alternate approach to the synthesis of a Ni(II) complex with pro-ligand [**L^{et}H**]$^+$(BPh$_4$)$^-$ was to use an external base to deprotonate the imidazolium salt *in situ* prior to addition of the nickel precursor (Ni(PPh$_3$)$_2$Cl$_2$). Triethylamine, potassium carbonate and potassium hexamethyl-disilazide (KHMDS) were all tested as bases for this reaction, however only KHMDS proved successful at deprotonating [**L^{et}H**]$^+$(BPh$_4$)$^-$. Thus, the precursor Ni(PPh$_3$)$_2$Cl$_2$ was reacted with ligand [**L^{et}H**]$^+$(BPh$_4$)$^-$ in the presence of excess KHMDS producing *bis*-ligated complex [**L$^{et}_2$Ni(II)**]$^+$(BPh$_4$)$^-_2$ as a yellow solid in 18% yield (Scheme 1b). We had hoped to generate a *mono*-ligated Ni(II) complex rather than the *bis*-ligated species due to our anticipation that a *bis*-ligated complex would be an inferior catalyst. Many attempts were made to improve the yield of complex [**L$^{et}_2$Ni(II)**]$^+$(BPh$_4$)$^-_2$ and to produce a *mono*-ligated complex, such as altering the reaction temperatures or ligand to metal ratios. However, any deviations from the synthetic method shown in Scheme 1b resulted in unsuccessful reactions which did not show evidence of any isolable species.

The ^{1}H NMR spectrum of the nickel(II) complex [**L$^{et}_2$Ni(II)**]$^+$(BPh$_4$)$^-_2$ revealed that the complex existed as an asymmetric species in solution. The ^{1}H NMR spectrum contained 19 distinct resonances, 16 of which were assigned to the protons of two ligands which suggested the complex had two NHC donors. The analysis of the NMR spectrum indicated that each ligand of complex

$[\mathbf{L^{et}_2Ni(II)}]^+(BPh_4)^-_2$ coordinated through only two donors, and that there was one non-coordinated pyrazolyl arm giving rise to the unsymmetrical structure. The ratio of the integrals of resonances due to the ligand and counterions indicates that the ratio of ligand to BPh_4 is 2:2, again indicating a likely *bis*-ligated complex. The absence of PPh_3 resonances in the ^{1}H NMR spectra of complex $[\mathbf{L^{et}_2Ni(II)}]^+(BPh_4)^-_2$ indicated that the two phosphine co-ligands have been displaced from the nickel centre and gave further credence to the proposal of a *bis*-ligated complex. Further analysis of $[\mathbf{L^{et}_2Ni(II)}]^+(BPh_4)^-_2$ by variable temperature ^{1}H NMR spectroscopy revealed that the resonance of one of the ethylene hydrogens was shifted to higher ppm at lower temperatures; perhaps indicating a strong C-H π-interaction with a pyrazolyl unit on the second ligand, see Fig. 7.
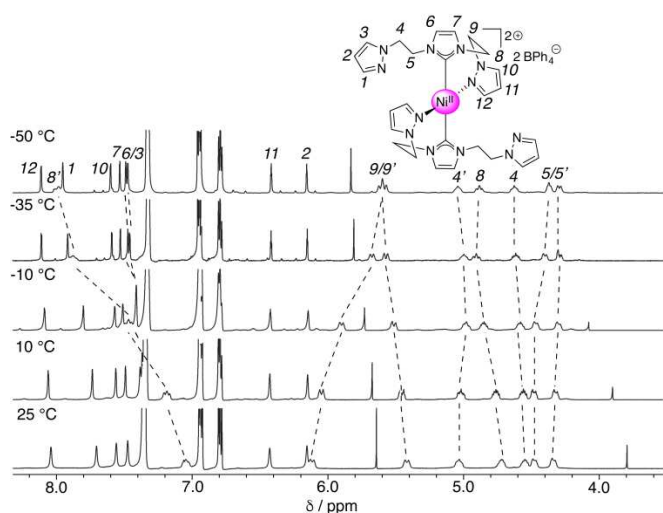
Fig 7. Variable temperature ^{1}H NMR spectra (600 MHz, $(CD_3)_2CO$) of complex $[\mathbf{L^{et}_2Ni(II)}]^+(BPh_4)^-_2$. ' in the ^{1}H NMR spectra denotes that an individual ^{1}H resonance is shifted due to interaction with the opposite ligand. Assignments correspond to the labelling shown in the figure.

Crystals of $[\mathbf{L^{et}_2Ni(II)}]^+(BPh_4)^-_2$ suitable for X-ray analysis were grown by vapour diffusion of diethyl ether into a saturated solution of $[\mathbf{L^{et}_2Ni(II)}]^+(BPh_4)^-_2$ in acetone. X-ray crystal structure analysis revealed that Ni(II) had a square planar geometry, with two ligands coordinated in a bidentate fashion through their carbene carbon and pyrazolyl nitrogen atoms (κ_2-*CN*) forming a homoleptic complex, see Fig. 8. The solid-state structure backs up our conclusions drawn from the

^{1}H NMR analysis. The significant shift of the resonances due to H[8'] to higher ppm ranges as observed in ^{1}H NMR was confirmed by X-ray analysis to be due to C-H π-interaction of the proton to a pyrazolyl ring with a distance of 2.845 Å. This distance is typical of C-H π-interactions of hydrogen atoms to an aryl ring.[32] A similar *bis*-ligated Ir(I) complex containing ligand $\mathbf{L^{et}}$ was reported previously by us, where the two ligands were located *trans* to each other.[24] However, $[\mathbf{L^{et}_2Ni(II)}]^+(BPh_4)^-_2$ shows a bidentate coordination of the ligand $\mathbf{L^{et}}$ to the metal centre whereas the Ir(I) counterpart had a monodentate coordination of the ligand to the metal centre. The solid state structure of $[\mathbf{L^{et}_2Ni(II)}]^+(BPh_4)^-_2$ confirmed our suspicion that access to the metal centre is severely hindered due the two organic ligands, this may have detrimental effects on catalysis activity.
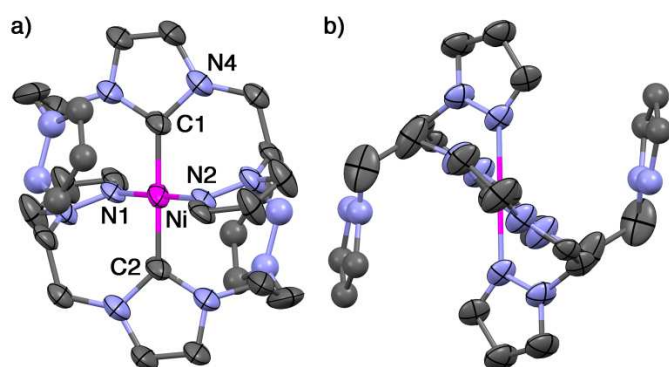
Fig. 8 X-ray crystal structure of $[\mathbf{L^{et}_2Ni(II)}]^+(BPh_4)^-_2$ as viewed (a) straight on and (b) viewed down C1-Ni-C2 axis. Ellipsoids are shown at the 50% probability level, hydrogen atoms and the two BPh$_4$ anions have been omitted for clarity.

3.4   Comparison of X-ray Crystal Structures

All three Ni(II) complexes, $[\mathbf{L^{me}Ni(II)Cl}]^+(BPh_4)^-$, $[\mathbf{L^{me}Ni(II)Cl}]^+(PF_6)^-$ and $[\mathbf{L^{et}_2Ni(II)}]^+(BPh_4)^-_2$, adopt a square planar geometry. The main difference between the structures of the complexes is that there are two ligands bound to the Ni(II) centre in a bidentate coordination mode in complex $[\mathbf{L^{et}_2Ni(II)}]^+(BPh_4)^-_2$ (Fig. 8) whereas there is only one ligand coordinated to Ni(II) in $[\mathbf{L^{me}Ni(II)Cl}]^+(BPh_4)^-$ (Fig. 2) and $[\mathbf{L^{me}Ni(II)Cl}]^+(PF_6)^-$ (Fig. 6). This is clearly as a result of the extra CH$_2$ in the linker between carbene and pyrazole (methylene *vs* ethylene). The bond lengths of

the inner coordination sphere of complexes [**L^{me}Ni(II)Cl**]$^+$(BPh$_4$)$^-$ and [**L^{me}Ni(II)Cl**]$^+$(PF$_6$)$^-$ are nearly identical as expected due to their isostructural solid state structures. Analogous Ni(II) square planar carbene complexes in the literature where a NHC ligand contains pendant pyridyl arms have similar Ni(II)-carbene (1.837 Å) and Ni(II)-Cl (2.236 Å) bond lengths to those of complexes [**L^{me}Ni(II)Cl**]$^+$(BPh$_4$)$^-$ and [**L^{me}Ni(II)Cl**]$^+$(PF$_6$)$^-$.[30] The Ni(II)-carbene bond length in complex [**L$^{et}_2$Ni(II)**]$^+$(BPh$_4$)$^-_2$ is slightly longer than that observed for [**L^{me}Ni(II)Cl**]$^+$(BPh$_4$)$^-$ and [**L^{me}Ni(II)Cl**]$^+$(PF$_6$)$^-$. As all three complexes consist of two pyrazolyl groups *trans* to each other, the Ni(1)-N(1) and Ni(1)-N(2) bond lengths are similar in all three complexes; the maximum variation in Ni(1)-N bond lengths is 0.012 Å. The two carbene carbons (C1 and C2) and two pyrazolyl nitrogens (N1 and N2) in complex [**L$^{et}_2$Ni(II)**]$^+$(BPh$_4$)$^-_2$ show no distortion from linearity as the Ni(II) ion lies at an inversion centre (C-Ni-C/N-Ni-N: 180.00(2)°). However, similar alignments in complexes [**L^{me}Ni(II)Cl**]$^+$(BPh$_4$)$^-$ and [**L^{me}Ni(II)Cl**]$^+$(PF$_6$)$^-$ exhibit slight distortion from linearity [**L^{me}Ni(II)Cl**]$^+$(BPh$_4$)$^-$: N-Ni-N: 176.02(2)°, [**L^{me}Ni(II)Cl**]$^+$(PF$_6$)$^-$: N-Ni-N: 178.88(2)°) which is likely due to strain arising from the tridentate coordination mode of **L^{me}**. There are also significant rotations of the NHC ligands out of the square plane in all three complexes, giving a torsion angle (N2-Ni-C1-Imidazolium N4) of 33° in complex [**L^{me}Ni(II)Cl**]$^+$(BPh$_4$)$^-$ and 30° [**L^{me}Ni(II)Cl**]$^+$(PF$_6$)$^-$ and 59° in complex [**L$^{et}_2$Ni(II)**]$^+$(BPh$_4$)$^-_2$.

Table 1 Selected bond lengths (Å) and angles (°) for [**L^{me}Ni(II)Cl**]$^+$(BPh$_4$, [**L^{me}Ni(II)Cl**]$^+$(PF$_6$)$^-$ and [**L$^{et}_2$Ni(II)**]$^+$(BPh$_4$)$_2$.

	Atoms	[**L^{me}Ni(II)Cl**]$^+$(BPh$_4$)$^-$	[**L^{me}Ni(II)Cl**]$^+$(PF$_6$)$^-$	[**L$^{et}_2$Ni(II)**]$^+$(BPh$_4$)$^-_2$
Bond lengths	Ni-C1	1.850(4)	1.847(2)	1.804(1)
	Ni-C2	----	-----	1.804(1)
	Ni-N1	1.908(3)	1.902(2)	1.995(8)
	Ni-N2	1.887(3)	1.900(2)	1.995(8)
	Ni-Cl	2.200(1)	2.220(1)	-----
Bond angles	C1-Ni-N1	89.8(2)	88.4(1)	91.6(2)

C1-Ni-N2	88.2(2)	88.6(1)	88.4(2)
C1-Ni-Cl	176.03(2)	178.88(2)	----
C1-Ni-C2	----	----	180.00(2)
N1-Ni-N2	177.10(2)	175.68(2)	180.00(2)

4. Catalytic Activity of Ni(II) Complexes for Kumada Cross Coupling of Aryl Halides

Ni(II) complexes are known to be efficient catalysts for the Kumada cross coupling reaction. Among the best nickel catalyst systems for the Kumada cross coupling reaction include nickel ions complexed to calixarene ligands. These catalytic systems achieve complete conversions of substrate at room temperature within 1 h, and can catalyse the reaction at low catalyst loadings (0.1-0.02 mol%).[33, 34] However, only a few Ni complexes of weakly coordinating ligands maintain high activity at elevated temperatures without suffering catalyst decomposition.[15] Thus, our complexes [L^{me}Ni(II)Cl]$^{+}$(BPh$_4$), [L^{me}Ni(II)Cl]$^{+}$(PF$_6$)$^{-}$ and [L^{et}_2Ni(II)]$^{+}$(BPh$_4$)$^{-}_2$ based on hemilabile ligands were evaluated as catalysts for the Kumada cross coupling reaction of aryl halides.

4.1 Catalytic Screen for Kumada Cross Coupling Reactions of Chlorobenzene and Bromobenzene.

Complexes [L^{me}Ni(II)Cl]$^{+}$(BPh$_4$)$^{-}$, [L^{me}Ni(II)Cl]$^{+}$(PF$_6$)$^{-}$ and [L^{et}_2Ni(II)]$^{2+}$(BPh$_4$)$^{-}_2$ were initially tested as catalysts for the Kumada cross coupling reactions of chlorobenzene and bromobenzene with phenylmagnesium bromide (Table 2).

Table 2 Kumada cross coupling reactions of PhBr and PhCl with PhMgBr catalysed by [$L^{me}Ni(II)Cl]^+(BPh_4)^-$, [$L^{me}Ni(II)Cl]^+(PF_6)^-$ and [$L^{et}_2Ni(II)]^{2+}(BPh_4)^-_2$.
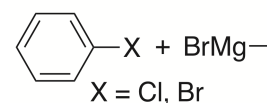
entry	substrate	catalyst	%conv. (3.5 h)
1		[$L^{me}Ni(II)Cl]^+(BPh_4)^-$	87 (80)[*]
2	Br	[$L^{me}Ni(II)Cl]^+(PF_6)^-$	90
3		[$L^{et}_2Ni(II)]^{2+}(BPh_4)^-_2$	41
4		[$L^{me}Ni(II)Cl]^+(BPh_4)^-$	>99 (43)[*]
5	Cl	[$L^{me}Ni(II)Cl]^+(PF_6)^-$	40
6		[$L^{et}_2Ni(II)]^{2+}(BPh_4)^-_2$	39

Reagents and conditions: Aryl halide (0.5 mmol), phenylmagnesiumbromide (1.5 mmol), catalyst (2 mol%), THF, 25 °C. [*] 1 mol% catalyst. %Conversions analysed at 3.5 h using GC-MS.

Complex [$L^{et}_2Ni(II)]^{2+}(BPh_4)^-_2$ proved to be the least active catalyst of the three catalysts tested, achieving only 40% conversion after 3.5 h of both chlorobenzene and bromobenzene (Table 2, entries 3 and 6). In comparison both [$L^{me}Ni(II)Cl]^+(BPh_4)^-$ and [$L^{me}Ni(II)Cl]^+(PF_6)$ gave more than double the conversion after the same reaction time. The low activity of complex [$L^{et}_2Ni(II)]^{2+}(BPh_4)^-_2$ is likely due to its coordinative saturation, as the Ni(II) centre is ligated by two of the ethylene containing ligands, L^{Et}. Any conversion of substrate promoted by [$L^{et}_2Ni(II)]^+(BPh_4)^-_2$ likely occurred due to the lability of the weakly coordinating pyrazolyl groups, allowing substrate access to the active metal centre. The pyrazolyl groups are positioned trans to each other along with the central NHC groups. Previous work reported in the literature has demonstrated that nickel bis-carbenic systems have reduced activity for the Kumada cross coupling reaction in relation to mono-carbenic systems.[35]

Complex [**L**^{me}**Ni(II)Cl**]$^+$(BPh$_4$)$^-$ proved to be the most effective catalyst overall for the Kumada cross coupling reactions of chlorobenzene and bromobenzene, achieving high conversions for both substrates after 3.5 h (Table 2, entries 1 and 4). The BPh$_4$ anion gives similar performance to PF$_6$ when using bromobenzene but when chlorobenzene was used the conversion was more than doubled. This was attributed to the lower coordinating ability of BPh$_4$$^-$ as a counterion than that of PF$_6$$^-$, which typically leads to higher catalyst efficiency.[31, 36] Due to the high conversions achieved using [**L**^{me}**Ni(II)Cl**]$^+$(BPh$_4$)$^-$, the reactions were repeated at a lower catalyst loading of 1 mol% to determine whether the catalyst maintains the activity at a lower loading. Whilst the conversion of bromobenzene only suffered a slight decrease in conversion, the conversion of chlorobenzene halved (Table 2, * entries).

4.2   Substrate scope of Kumada cross coupling reaction using [**L**^{me}**Ni(II)Cl**]$^+$(BPh$_4$)$^-$

As complex [**L**^{me}**Ni(II)Cl**]$^+$(BPh$_4$)$^-$ proved to be the most effective catalyst under investigation here for the cross coupling reactions of bromobenzene and chlorobenzene, it was tested as a catalyst for the transformation of a selection of substrates with phenylmagnesiumbromide (Table 3). We elected to use a catalyst loading of 2 mol%, as this gave the best conversion. Unsurprisingly, iodobenzene gave quantitative conversion to biphenyl product. Of all the substrates featuring a substituent that were tested for conversion to biphenyl products using [**L**^{me}**Ni(II)Cl**]$^+$(BPh$_4$)$^-$, the highest conversion was achieved for the substrate containing an electron withdrawing *para*-CF$_3$ substituent on the aryl ring (90%). However, the substrate with two *meta*-CF$_3$ groups gave only 68% conversion. Disappointingly, *para*-cyanochlorobenzene gave no conversion to product. In comparison, substrates with electron donating substituents (*i.e.* methoxy and methyl) gave lower conversion to products. It was interesting to observe that the choice of halide altered the selectivity of cross coupling reactions to form biphenyl or triphenyl products. The catalysed reaction of phenylmagnesium bromide with the 1,3-dibromobenzene resulted in selective formation of the monosubstituted 1-bromo-3-phenylbenzene. However, the catalysed reaction of the analogous 1,3-

dichlorobenzene with phenylmagnesium bromide results in the selective production of the disubstituted 1,3-diphenylbenzene, although the yield was low. This result was unexpected considering 1,3-dibromobenzene is more likely to produce the disubstituted product due to the propensity of bromide groups to be more readily substituted in comparison to chloride groups.

Table 3 Range of substrates catalysed by [**L^{me}Ni(II)Cl**]$^{+}$(BPh$_4$)$^{-}$ in Kumada cross coupling reactions.

entry	R-X	% conv.	entry	R-X	% conv.
1	Ph–I	>99	5	F$_3$C–C$_6$H$_4$–Br	90
2	CH$_3$–C$_6$H$_4$–Br	78	6	1,3-dibromobenzene	67 (mono)
3	CH$_3$O–C$_6$H$_4$–Br	50	7	1,3-dichlorobenzene	16 (di)
4	2,4-(F$_3$C)$_2$–C$_6$H$_3$–Br	68	8	NC–C$_6$H$_4$–Cl	0

Reagents and conditions: Aryl halide (0.5 mmol), phenylmagnesiumbromide (1.5 mmol), catalyst (2 mol%), THF, 25 °C. %Conversions analysed at 4 h using GC-MS. (m = mono-substituted product, d= di-substituted product).

Overall, our nickel(II) catalyst [**L^{me}Ni(II)Cl**]$^{+}$(BPh$_4$)$^{-}$ has proved to be an effective catalyst for the room temperature Kumada cross coupling. Complete conversion of iodobenzene and chlorobenzene was observed after just 4 hours at room temperature. This places this catalyst above the NHC-Ni(II) catalysis reports from Wang[11, 15] and Louie (though mesitylmagnesium bromide was used).[35] The levels of conversion of substituted aryl-halides obtained using catalyst [**L^{me}Ni(II)Cl**]$^{+}$(BPh$_4$)$^{-}$ were slightly less than those reported by Wang.[15] The activity of our

catalysts is similar to that reported by Semeril and Matt observed using their calixarene-based Ni(II) catalysts.[33, 34]

5. Conclusions

Here, we synthesized three Ni(II) complexes using ligands containing both carbene and pyrazolyl donor groups with either a methylene or ethylene linker joining the pendant pyrazolyls to the central carbene group. The Ni(II) complexes featuring the shorter methylene linker, $[\mathbf{L^{me}Ni(II)Cl}]^{+}(\mathrm{BPh_4})^{-}$ and $[\mathbf{L^{me}Ni(II)Cl}]^{+}(\mathrm{PF_6})^{-}$, had similar solid-state structures. The complex with the $\mathrm{BPh_4}^{-}$ counterion outperformed the $\mathrm{PF_6}^{-}$ analogue when used for the Kumada catalysis reactions, which has been attributed to the weaker coordination of the $\mathrm{BPh_4}^{-}$ counterion. The Ni(II) complex of the longer ethylene linker, $[\mathbf{L^{et}_2Ni(II)}]^{+}(\mathrm{BPh_4})^{-}_2$, was found to have limited catalytic activity due to the coordinative saturation of the complex, as shown in its solid-state crystal structure. Complex $[\mathbf{L^{me}Ni(II)Cl}]^{+}(\mathrm{BPh_4})^{-}$ was found to be the most active catalyst, it proved compatible with different functional groups and performed more difficult di-substitution reactions. Excellent to moderate yields were achieved in the Kumada cross coupling reactions at room temperature with substrates containing electrodonating substituents. Thus, complex $[\mathbf{L^{me}Ni(II)Cl}]^{+}(\mathrm{BPh_4})^{-}$ was found to be a good general catalyst for the Kumada cross coupling reaction.

6. Acknowledgements

7. References

[1] K. Tamao, K. Sumitani, M. Kumada, J. Am. Chem. Soc., 94 (1972) 4374-4376.

[2] R.J.P. Corriu, J.P. Masse, J. Chem. Soc., Chem. Commun., (1972) 144a-144a.

[3] A.H. Cherney, N.T. Kadunce, S.E. Reisman, Chem. Rev., 115 (2015) 9587-9652.

[4] N. Miyaura, K. Yamada, A. Suzuki, Tetrahedron Lett., 20 (1979) 3437-3440.

[5] S. Baba, E. Negishi, J. Am. Chem. Soc., 98 (1976) 6729-6731.

[6] P. Spannring, I. Reile, M. Emondts, P.P.M. Schleker, N.K.J. Hermkens, N.G.J. van der Zwaluw, B.J.A. van Weerdenburg, P. Tinnemans, M. Tessari, B. Blümich, F.P.J.T. Rutjes, M.C. Feiters, Chem. Eur. J., 22 (2016) 9277-9282.

[7] D. Milstein, J.K. Stille, J. Am. Chem. Soc., 100 (1978) 3636-3638.

[8] D. Milstein, J.K. Stille, J. Am. Chem. Soc., 101 (1979) 4992-4998.

[9] J.K. Stille, Angew. Chem. Int. Ed., 25 (1986) 508-524.

[10] K. Sonogashira, Y. Tohda, N. Hagihara, Tetrahedron Lett., 16 (1975) 4467-4470.

[11] Z.-X. Wang, N. Liu, Eur. J. Inorg. Chem., 2012 (2012) 901-911.

[12] T. Kohei, S. Koji, K. Yoshihisa, Z. Michio, F. Akira, K. Shun-ichi, N. Isao, M. Akio, K. Makoto, Bull. Chem. Soc. Jpn., 49 (1976) 1958-1969.

[13] S. Lou, G.C. Fu, J. Am. Chem. Soc., 132 (2010) 1264-1266.

[14] C.E.I. Knappke, A. Jacobi von Wangelin, Chem. Soc. Rev., 40 (2011) 4948-4962.

[15] C. Zhang, Z.-X. Wang, Organometallics, 28 (2009) 6507-6514.

[16] P.M. Perez Garcia, T. Di Franco, A. Epenoy, R. Scopelliti, X. Hu, ACS Catal., 6 (2016) 258-261.

[17] M.H.P. Rietveld, D.M. Grove, G. van Koten, New J. Chem., 21 (1997) 751-771.

[18] D. Morales-Morales, C. Jensen, The Chemistry of Pincer Compounds, 1st ed., Elsevier, 2007.

[19] N. Selander, K. J. Szabó, Chem. Rev., 111 (2011) 2048-2076.

[20] J.I. van der Vlugt, J.N.H. Reek, Angew. Chem. Int. Ed., 48 (2009) 8832-8846.

[21] A. de Meijere, F. Diederich, Metal-Catalyzed Cross-Coupling Reactions, 2nd ed., Wiley, 2004.

[22] C. Chen, H. Qiu, W. Chen, J. Organomet. Chem., 696 (2012) 4166-4172.

[23] R. Wang, Z. Zeng, B. Twamley, M.M. Piekarski, J.M. Shreeve, Eur. J. Org. Chem., 2007 (2007) 655-661.

[24] G. Mancano, M.J. Page, M. Bhadbhade, B.A. Messerle, Inorg. Chem., 53 (2014) 10159-10170.

[25] A.G. Nair, R.T. McBurney, D.B. Walker, M.J. Page, M.R.D. Gatus, M. Bhadbhade, B.A. Messerle, Dalton Trans., 45 (2016) 14335-14342.

[26] B. Corain, B. Longato, R. Angeletti, G. Valle, Inorganica Chimica Acta, 104 (1985) 15-18.

[27] L. Brammer, E.D. Stevens, Acta Crystallographica Section C, 45 (1989) 400-403.

[28] Advanced Inorganic Chemistry, 5th ed., John Wiley and Sons, New York, 1988.

[29] D.F. Evans, Journal of the Chemical Society (Resumed), (1959) 2003-2005.

[30] E.M. Schubert, Journal of Chemical Education, 69 (1992) 62.

[31] M. Jia, M. Bandini, ACS Catal., 5 (2015) 1638-1652.

[32] H. Suezawa, S. Ishihara, Y. Umezawa, S. Tsuboyama, M. Nishio, Eur. J. Org. Chem., 2004 (2004) 4816-4822.

[33] D. Sémeril, M. Lejeune, C. Jeunesse, D. Matt, Journal of Molecular Catalysis A: Chemical, 239 (2005) 257-262.

[34] L. Monnereau, D. Sémeril, D. Matt, Adv. Syn. Catal., 355 (2013) 1351-1360.

[35] K. Zhang, M. Conda-Sheridan, S. R. Cooke, J. Louie, Organometallics, 30 (2011) 2546-2552.

[36] G. Ciancaleoni, L. Belpassi, D. Zuccaccia, F. Tarantelli, P. Belanzoni, ACS Catal., 5 (2015) 803-814.

Highlights

- Three Ni(II) complexes have been synthesised from a carbene-bis-pyrazole ligand.
- The complexes all exhibited a square-planar coordination geometry.
- The complexes acted as catalysts in Kumada cross coupling reactions.